Yeast RNAi Machinery Maintains rRNA Homeostasis for Ribosomal Function by Generating sirRNAs to Suppress the Antisense Transcripts

Chenxi Li
College of Life Sciences, Beijing Normal University
Ping Zhang
College of Life Sciences, Beijing Normal University
Liang Huo
College of Life Sciences, Beijing Normal University
Xiaoyu Ma
College of Life Sciences, Beijing Normal University
Xiaoran Hao
College of Life Sciences, Beijing Normal University
Lan Ma
College of Life Sciences, Beijing Normal University
Yanjie Liu
College of Life Sciences, Beijing Normal University
Mengkai Zhou
College of Life Sciences, Beijing Normal University
Xudong Zhu (zhu11187@bnu.edu.cn)
College of Life Sciences, Beijing Normal University https://orcid.org/0000-0001-8790-2012

Article

Keywords: RNAi, rRNAs, sirRNAs, non-coding sRNAs, Cryptococcus neoformans

Posted Date: March 24th, 2022

DOI: https://doi.org/10.21203/rs.3.rs-1429690/v1

Abstract

The biological function of RNAi machinery in fungi appears puzzling. In yeast *Cryptococcus neoformans*, we observed that RNAi-deficient mutants displayed diminished ribosome function. We conducted deep sequencing and bioinformatics analysis for siRNAs derived from rRNAs (sirRNAs), and discovered a novel class of sirRNAs with unique structure, *e.g.* a nucleotide C at 5'end, and a size of 19 or 20 nt. Two sirRNAs, 001 and 006, had the largest reads of all sRNAs and were located on 25S rRNA close to each other with a 4-nt spacer. Sequencing data and Northern blotting manifested sirRNAs were generated by RNAi machinery, rather by random degradation. Multiple RNAi pathways could produce sirRNAs, a long pathway consisting of Dcrs, Agos and Rdp and a short pathway through Dcrs and Agos solely. We found a 120-nt 25S rRNA fragment was the common precursor of sirRNAs 001/006 which were split into two pri-sirRNAs, 55-nt and 60-nt, respectively. The pri-sirRNAs were further processed merely by RNAi machinery to form pre-sirRNAs, subsequently the final products sirRNAs 001 and 006. Silencing assays suggested that sirRNAs-guided RNAi suppressed the expression of the reporters, *URA5* and *CLC1*. On the other hand, we found loss of RNAi caused a significant decrease of 25S rRNA, but a dramatically increase of the natural antisense transcripts of rRNAs (NAT-rRNAs), suggesting RNAi machinery played a positive role in maintaining 25S rRNA level, while an antagonistic suppression on NAT-rRNAs which was demonstrated by sequencing and blotting. Considering the presence of sirRNAs, we speculate the yeast has evolved a protective mechanism for rRNA homeostasis through sirRNAs-guided RNAi against NAT-rRNAs. When RNAi machinery was absent, NAT-rRNAs were accumulated to form with rRNAs double-stranded RNA molecules and caused rRNAs to be degraded, which impaired ribosomal function. This work reveals that RNAi machinery maintains rRNA homeostasis and ribosome function.

Introduction

RNA interference (RNAi) was initially used to explain gene silencing caused by introduction of foreign dsRNA into *Caenorhabditis elegans* (1, 5, 7). The fundamental of RNAi also centers the biogenesis of endogenous siRNAs and siRNAs-guided gene expression regulation (5, 7). Conventional RNAi machinery contains three core proteins, *i.e.* the RNase III ribonuclease Dicers, which cleave double-stranded RNAs (dsRNAs) to generate 18-25-nt siRNAs; the effector Argonaute proteins that are guided by produced siRNAs to implement the step of gene silencing on the complementary targets (1, 7). And often an RNA-dependent RNA polymerase (Rdp) is required in many organisms (8, 17). The regulation of gene expression guided by endogenous siRNAs can occur at various stages of gene expression, for instance, methylation of DNA in the plants (9, 36), and heterochromatin in the fission yeast (26), the knock down on the target mRNAs at the post-transcriptional stage, and regulation of translation process (1, 33). As a result, intracellular siRNAs/RNAi machinery defends the integrity of genome by inhibiting the action of selfish nucleic acids such as transposons and modulates the growth and development in complex organisms (1, 5, 7). Especially, RNAi machinery participates in scavenging of abnormal dsRNAs formed under stress conditions (3), *e.g.* by DNA damages in *Neurospora crassa* (22), or by abnormal splicing in *Cryptococcus neoformans* var. *grubii* (12). Recent findings include the trans-kingdom siRNAs-mediated

RNAi in phytopathogenic fungi which modulates the host gene expression, shaping a novel type of pathogen-host communication (16, 29).

The widely applied high throughput sequencing technique (HT-seq) has greatly expedited the characterization of endogenous siRNAs and made feasible to clarify the origination sources of them from the acting targets. HT-seq projects have revealed a large number and variegated originating sources of siRNAs, including transposable elements, repeated regions, intergenic region and even protein encoding genes (5, 7). Unfortunately, siRNAs derived from rRNAs have been neglected and are often considered random debris of rRNA degradation, thus usually abandoned in bioinformatics analysis (19, 32, 34, 35). As a matter of fact, there are indeed a large number of small rRNA fragments derived from rRNA degradation (3,11,19,24, this study). Several rRNA-derived sRNAs, ITS region or the antisense rRNAs (often 20–30 nt) have been described, *e.g.* in the fission yeast *Schizosaccharomyces pombe*, fly, zebra fish, wheat, mouse and human (reviewed in 20). However, the reality of them are still under disputation (20), considering that they are protected by heavy modifications and associated with ribosomal proteins (13). Thus, the issues, *e.g.* whether rRNAs could be the substrates of RNAi machinery to make sirRNAs is still not clearly defined. And the biological significance of found sirRNAs, if they are real siRNAs, may need to be reconciled (7, 20).

RNAi machinery in fungi, though evolutionarily conserved, shows subtly distinct in many aspects compared to the counterparts in complex organisms (6, 25). For instance, the miRNA equivalents have not been clearly defined in fungi. Many fungi have lost the RNAi pathways, *e.g. Saccharomyces cerevisiae* (10, 11). In some, if not all, extant RNAi pathways are dispensable for growth and differentiation at least under the normal laboratory condition (6, 17, 25). The conventional endogenous siRNAs, 20–25 in length, with a U at the 5', are reported in fungal kingdom, but indeed exhibit little conservation in sequence or function. Thus, to understand fundamentals about RNAi, *e.g.*, the evolutionary rise of RNAi, investigation in fungi is of significance.

The basidiomycetous yeast *Cryptococcus neoformans* is an opportunistic pathogen, yet widely exists as a saprophyte in soil. It contains two dicer homologs, two Argonautes, and one Rdp and performs transgene-evoked RNAi (17). RNAi machinery is involved in a process of sex-induced transgenic silencing (SIS) (27), and degradation of mis-spliced mRNAs in *C. neoformans* var. *grubii* H99 (4, 12). RNAi machinery plays a role in suppression of transposons in var. *neoformans* (17). Likewise, the pathways in this fungus are dispensable. Disruption of the RNAi pathways renders little influence on the growth or pathogenicity, stress tolerance and the hypersensitivity to DNA damaging agents (Fig.S1A) (17).

To find out the selection cause for RNAi pathways in this yeast, we conducted extensive search for the phenotypic changes in the RNAi-deficient mutants. Interestingly, we found that RNAi mutants displayed severe hypersensitivity to several ribosomal inhibitors, *e.g.* G418 and hygromycin B. We deduced that RNAi machinery was most likely involved in the metabolism of rRNAs. We hence conducted high throughput sequencing (HT-seq) and bioinformatics analysis for rRNA-derived siRNAs (sirRNAs). HT-seq disclosed the presence of both novel sRNAs from rRNAs (designated as sirRNAs), as well as a population

of the classic siRNAs corresponding to the antisense transcripts of rDNA loci (designated as NAT-rRNAs). Two of the sirRNAs, sirRNAs 001 and 006, located on the internal region of 25S rRNA, had the greatest reads of all classes in HT-seq and high abundance in Northern blots. We demonstrated they were products of the RNAi machinery, rather than random degradation. Importantly, we found RNAi machinery were critical in maintenance of 25S rRNA homeostasis and the normal function of ribosomes, by suppression of NAT-rRNAs. We here present the detailed results.

Results

Sensitivity of RNAi-deficient mutants to ribosomal inhibitors

Utilizing the disruption mutant strains corresponding to the five genes encoding the members in the RNAi machinery (17), we extended the search for phenotypic consequence from the disruption. We found that, compared to the wild type, RNAi mutants were hypersensitive to inhibitory chemicals of eukaryotic ribosomes, *e.g.*, hygromycin B, G418 and anisomycin, suggesting impairments in the ribosomes (Fig. 1A-C). The mutant strains exhibited significantly delayed growth on the plates supplemented with the drugs. This result indicates that there were defects in the ribosome function resulted from the loss of RNAi machinery. Considering the action of RNAi machinery, we turned to examine the rRNA level to find out whether sirRNAs were produced in the yeast.

Abundant sRNAs generated in *C. neoformans* and a novel class of rRNA-derived sRNAs

Using PAGE, we observed that JEC21 actually produced a large amount of 20-25-nt sRNAs (WT, Fig. 1D). This unique capacity of sRNAs production is rarely seen, even in some other RNAi-proficient fungi (Fig. S1B). Relying on the RNAi-deficient mutants of JEC21, we clearly witnessed that the biogenesis of 20-25-nt sRNAs in the yeast was dependent on the function of RNAi machinery (Fig. 1D). Disruption of the components of the pathways led to a significant drop of sRNAs. Thus they are siRNAs in general. The largest decrease in the amount of siRNAs was seen in three mutants, *rdp1Δ*, *ago1Δ* (CNJ00490) and *dcr1Δ*. Thus, Rdp1, Ago1 and Dcr1 possibly played a major part in the generation of endogenous siRNAs in JEC21. This pathway is divergent from the conventional transgene-evoked RNAi pathway in JEC21 *i.e.* Dcr2, Rdp1 and Ago1 play a major role (14), which is also the SIS pathway in var. *grubii* strain H99 (27). Notably, a trace, yet discernable amount of siRNAs was left in the double mutant, *dcr1△dcr2△*, suggesting unidentified pathways, *e.g.* the RNase IIIs apart from the Dicers, such as Rnt1, were capable to generate sRNAs as well (4,21).

To identify sirRNAs from the entire population of siRNAs, we conducted HT-seq followed by bioinformatics covering all 18-30-nt sRNAs with emphasis on sirRNAs in that range. A chart on relative percentages of siRNAs sorted by origination sources was depicted in Figure 2A, which displayed a diversity of siRNA originations in *C. neoformans*. A group of siRNAs from transposable elements took the largest percentage, up to 72.59%, of all groups (Left panel), similar to a previous observation in var. *grubii* H99 (12,14,27). Surprisingly, a group of putative sirRNAs delimited by structural characteristics took the second position, up to 12.88%, of the entire sRNA population. In the control *rdp1Δ* (Right panel), the

percentage of all the non-sirRNAs dropped sharply to only 13.08%, whereas sirRNAs climbed to 86.92%. The shifting of percentages attests in consistence with the PAGE data that RNAi machinery plays a critical role in the biogenesis of endogenous siRNAs.

A routine analysis for the regular siRNAs (non-sirRNAs hereafter), in which sirRNAs were excluded, was separately conducted. The size allocation of them exhibited a range from 20 to 24 nt with a reads peak at 22 nt (~37%) (Left panel). A preference of nucleotide U at 5' end was obvious (Fig. 2C). These archetypal structural features demonstrate they are siRNAs of *C. neoformans*. The features were lost in *rdp1Δ*, suggesting they were largely the products of Rdp-dependent RNAi. In parallel, we conducted bioinformatics analysis for sirRNAs (Fig. 2B&C, Right panels). They were distinct from siRNAs in structure. The size allocation peaked at 19 and 20 nt, shorter than the siRNAs. They had a nucleotide preference of C at the 5' end (more than 95%), suggesting sirRNAs are a novel class of siRNAs. Such characteristic features disappeared in *rdp1Δ*, and again manifesting a role of Rdp1 in sirRNA biogenesis (Fig. 2, Fig.S2 and S3). Depiction on reads of sirRNAs verse the location on rRNA sequences revealed a pattern of clustered distribution, ascertained they were generated by RNAi machinery but not random degradation (Fig. 2D). We also found a large number of classic siRNAs corresponding to the antisense sequence of rDNA, suggesting they were derived from the natural antisense transcripts of rDNAs (NAT-rRNAs for short), thus, designated as a-sirRNAs for antisense sirRNAs (Fig. 2E). The presence of a-sirRNAs suggested that RNAi occurred on NAT-rRNAs. Taken together, we demonstrated the existence of RNAi-generated sirRNAs in *C. neoformans*, which are new in *C. neoformans*. And a-sirRNAs from NAT-rRNAs were also found. The co-existence of two classes of siRNAs derived from the complementary transcripts of the same genetic loci manifests complexity of RNAi in this yeast.

Characterization of sirRNAs 001/006 and their biogenesis by RNAi machinery

By HT-seq, we discovered two sirRNAs, 001 and 006, had the largest number of reads. They each had three isoforms sharing a similar sequence (Table 1). Alignment confirmed they were originated from 25S rRNA and largely Rdp-dependent (Fig. 2D, S4A). Interestingly, they were located in juxtaposition with a spacer of 4 nucleotides (Fig. 3A, S4A), and likely formed intracellular duplex to make substrate of the dicers (Fig. 3A). Computation predicted a possible stem-loop structure within a sequence of approximately 108-nt flanking the sirRNAs, 001/006, with an initial ΔG = -58.00 Kcal/mol (a minimal value of ΔG is 25 Kcal/mol for stem-loop formation). In the prediction, sequences of 001 and 006 could form perfect duplex to each other in inverted orientation, leaving a loop of the 4-nucleotide spacer. Non-Watson-Crick base pairing was employed in the stem, *e.g.* eight G-U and two A-A pairings in the twenty base-paired 001-006 duplex. G-U and A-A pairings are common in RNA molecules (13). However, whether this duplex could be a suitable substrate for dicing by RNase IIIs to generate sirRNAs 001/006 needs proof.

To demonstrate the existence of sirRNAs, we believed the HT-seq and bioinformatics data should further be confirmed by molecular approaches. We reasoned that bona fide sirRNAs should meet two criteria: 1) They should be at a stable concentration sufficient to promote RNAi reaction. 2) They should be

processed into an approximately uniform length, *i.e*, 20-25 nt, by RNAi, which made them distinguishable from degradation products. Therefore they could form clear bands that were visible in Northern blotting. To verify the results of HT-seq, we performed Northern blotting for sirRNAs 001/006. As expected, we saw strong signals of 001/006 in the wild type, especially in an extremely high and stable level (WT lane, Fig. 3B). This result clearly verified the presence of 001/006. In RNAi mutants, signals of 001/006 decreased greatly, confirming that the majority of them were produced by RNAi machinery (Fig. 3B). In the control blots for two rsRNAs 033 and 065 (locus shown in Fig.S4A), two randomly chosen small rRNA fragments (20-25 nt) also obtained by HT-seq, only smeared signals were detected, suggesting they were degraded rRNA fragments (Fig. S4C). Thus, rRNA-degraded sRNAs were indeed present and probably in a large number in the sequenced sRNAs. And they were difficult to be distinguished from the RNAi-dependent sRNAs only by HT-seq. Even more, a clear remainder band of 001 or 006 in *rdpΔ* (Fig. 3B), suggesting that a fair portion of sirRNAs 001/006 were made through an Rdp-independent pathway, likely by Dcr1/2 or other pathways. This result was consistent with the HT-seq data which showed that in *rdpΔ*, the reads of sirRNAs 001 dropped by 70.57%, while sirRNA-006 by 84.02%, verse the reads in the wild type JEC21 (Table 1). Blotting result still suggested that each individual member in the pathways, Dcr1, Dcr2, Ago1 or Ago2, was critical for the biogenesis of 001/006, as well as a precursor (approximately 33 nt for 001 and ~35 nt for 006, arrowed, Fig. 3B, 3C). Disruption of any one led to a significant decrease of 001/006 and the precursor, suggesting that the components of the machinery act in a manner of cooperation in the biogenesis process of sirRNAs. In sum, HT-seq and Northern blots clearly demonstrate the presence of a novel class of rRNA-derived sRNAs, sirRNAs in *C. neoformans*, and they are generated by RNAi machinery.

Unique mechanism of the biogenesis of sirRNAs

The above Northern blots suggested that the two Dcrs and the two Agos, plus Rdp could form a long pathway in the biogenesis of the majority of sirRNAs 001/006 (Fig. 3B). Reads data confirmed that a fair amount of sirRNA 001 (29.43%) and 006 (15.98%) remained in *Δrdp1* (Table 1). In other words, this portion of sirRNAs 001/006 could be produced by a short pathway without Rdp, *e.g.*. probably by the Dcrs with Agos (Lane *rdp1Δ*, Fig. 3B). Two other blots with double mutant strains, *dcr1dcr2* and *ago1ago2*, confirmed both Dcrs and Agos are involved in the short pathway (Fig.3C). Even more, when we disrupted two copies of Dcrs or Agos, we could still see a trace amount of sirRNAs 001 and 006 in the blots, suggesting a third pathway was acting (Fig.3C), which might contain other RNase IIIs in addition to the known Dcrs. In short, our data suggests at least three pathways could independently generate sirRNAs in the yeast.

Unlike mammalian cells, fungi have no counterparts of the microprocessor which consists of different set of proteins for the generation of miRNA precursors (1,5). To elicit the early steps leading to the production of sirRNAs, we explored the initial rRNA substrates and intermediate products. We constructed double mutants for the genes of the Dcrs and Agos, designated as *dcr1dcr2Δ* and *ago1ago2Δ*, respectively. Northern blots to detect the intermediate products in these strains were performed (Fig. 3C). In Fig. 3C (Lane WT, right panels), a band near 120 nt (by calculating the mobility with the markers) below the 25S rRNA band was respectively detected by the probes for sirRNAs 001 and 006, suggesting this band was a

shared precursor by sirRNAs 001 and 006, thus, designated as pro-sirRNAs. Below this band, processing of the precursor diverges into two distinct pathways toward the final sirRNAs. Generation of this 120-nt precursor was apparently independent of RNAi machinery, *i.e.* it was not a process of RNAi. As a matter of fact, disruption of Dcrs or Agos actually led a discernibly increase of the 120-nt precursor, rather than a decrease (indicated by arrow, Lanes *dcr1dcr2* and *ago1ago2*, Fig. 3C). Nonetheless, the RNAi machinery obviously participated in the following steps. This was evident by band pattern of intermediate products in-between of the 120-nt precursor and the sirRNAs in the mutants (Fig. 3C, Right panels). Along the route to sirRNAs 001, there were four bands, approximately, 80 nt, 70 nt, 55 nt and 33 nt (Lane WT), indicating four corresponding steps of processing. Whereas there were only two intermediates, 60 nt and 35 nt, leading to the generation of sirRNAs 006 (Lane WT, Fig. 3C). In RNAi mutants, these intermediate products significantly decreased or disappeared, demonstrating that Dcrs (1/2) and/or Agos (1/2) participated in generating these intermediates (Fig. 3B, C). Notably, there were still trackable amount of the intermediate products in the double mutants (Fig. 3C, Lanes *dcr1dcr2Δ* and *ago1ago2Δ*), suggesting that other pathways, *e.g.*, RNase IIIs, participate in the formation of the intermediate products. As the 55-nt and 60-nt bands for 001 and 006, respectively, exhibited as the major ones during this stage, thus designated them as pri-sirRNAs. Subsequently, we could see that Dcrs and Agos processed the pri-sirRNAs into two products, the 33-nt one for 001, and the 35-nt for 006 (Fig. 3B, C, Right two panels). We hereby designate these two small rRNA fragments as pre-sirRNAs. Last, the RNAi machinery was definitely required for the formation of the mature sirRNAs 001 and 006. In sum, our data suggests that the biogenesis of sirRNAs 001/006 could be roughly divided into three stages (Fig. 6C). The primary stage gives rise to a 120-nt rRNA precursor, the pro-sirRNAs, from rRNAs with an unknown mechanism. The second stage is the generation of pri-sirRNAs, the 55-nt product for 001 and the 60-nt for 006, by split of the 120-nt precursor. In this stage, RNAi machinery and a certain unidentified RNase IIIs are involved. The last stage is responsible for the formation of pre-sirRNAs and the final products sirRNAs 001 and 006. And this stage is accomplished solely by the RNAi machinery. Disruption of the two Dcrs or Agos led to a nearly complete loss of pre-sirRNAs and most sirRNAs (Fig. 3C). Still, we can see that Rdp played a critical role in the third stage. In *rpdΔ,* pre-sirRNAs were hardly detectable as in the double mutants (Fig. 3B), suggesting that sirRNAs were mainly generated from the products of Rdp amplification that were subject to processing by the Dcrs and Agos, rather than from a stem-loop precursor, or the double-stranded RNA molecules formed by rRNA and NAT-rRNAs (Fig. 6C).

In short, our experiments delimited that three potential pathways could contribute to the biogenesis of sirRNAs 001/006, the long one including Rdp, Dcrs and Agos, a short one containing merely Dcrs and Agos, and a third unidentified pathway. Rdp vastly boosts the yield of sirRNAs 001/006. This biogenesis mechanism of sirRNAs 001/006 is distinct from the known strategies of the biogenesis of siRNA or miRNA (1,5,7).

Silencing activity of sirRNAs 001/006

We reasoned whether an endogenous sirRNA had the capacity to effectively trigger RNAi reaction on targets might rely on two conditions, the first was the intracellular concentration of the sirRNA and

secondly their accessibility to RNAi machinery. We then tested whether sirRNAs 001/006 could guide RNAi machinery to knock down the expression of reporter genes. To this end, we employed a reporter cassette that was previously designed for silencing assay in *C. neoformans* JEC21 (28). The yeast genes *URA5* and *CLC1* were inserted with a complementary sequence of 001 or 006 to form the targets (Fig.4A). As expected, the transformants carrying the cassette of *URA5-sirRNAs* displayed retarded growth on minimal media YNB (Fig. 4B). Meanwhile they showed an apparent tolerance to the toxin 5-FOA (the right panel), demonstrating that expression of *URA5* was suppressed. The control strain which contained only the plasmid (*URA5*) grew properly on YNB, but failed to grow on FOA-containing plate (right panel). A following qPCR measurement confirmed a deep fall of *URA5* mRNA in the transformants (Fig.4C). Similarly, in the test for the cassette of *CLC1-sirRNAs* (Fig. 4D, Bottom panels), transformants of silencing cassette produced less pigments on nor-epinephrine (NE)-containing plates, which was similar to a *clc*-disrupted mutant TX1 (*clc1Δ*) (23), verifying a silencing effect on *CLC1*. A qPCR confirmed a significant decrease of *CLC1* mRNA in the transformants (Fig. 4E). Thus, sirRNAs, 001 and 006, could trigger RNAi reaction on the complementary targets and caused silencing effect. Also, this assay implies that sirRNAs could initiate RNAi against invasive nucleic acids.

RNAi machinery maintains 25S rRNA level by suppressing NAT-rRNAs

Considering the fact that a large sum of sirRNAs 001/006 were synthesized from 25S rRNAs, we reasoned that the level of 25S rRNA might rise when RNAi pathways were disrupted. To test this hypothesis, we applied qPCR to measure the level of 25S rRNA in RNAi mutants. Contrary to our expectation, the level of 25S rRNA decreased apparently in all mutants (Fig. 5A). For instance, the amount of 25S rRNA in *ago1Δ* was only ~56% of that in the wild type. Thus, the machinery rather played a positive role in maintaining the level of 25S rRNA. To explain this paradoxical result, we conceived that natural antisense transcripts (NAT-rRNAs) might be expressed from the repetitive rDNA loci that could form RNA duplex with rRNAs to cause rRNAs to be degraded by RNase IIIs or/and exosomes.

We searched for NAT-rRNAs arisen around the locus of sirRNAs 001/006 and detected them by reverse transcription PCR (Fig. S4D). We did Northern blots and qPCR to track the variation of the Nat-rRNA fragments in RNAi mutants. We knew that it was risky to expect a concentrated band of NAT-rRNAs in the blots, as NAT-rRNAs might be transcribed into fragments of various length. However, it is proven that RNAi in this yeast generates a 70-nt precursor of the targets which may accumulate in RNAi mutants (18). Hence, we probed instead the 70-nt precursor of NAT-rRNAs in the mutants. We conducted two blots in parallel with two probes, one located at the 001/006 locus (Table S2, Fig. S4E). The blots were shown in Fig. 5B. In the wild type, the NAT-rRNA band was barely seen, suggesting it was in a state of suppression by RNAi, if taking into account of a-sirRNAs in the wild type (Fig. 2E). In contrast, NAT-rRNAs remarkably mounted in all the mutants in dual blots. This result clearly verified that RNAi mediates the suppression of NAT-rRNAs in the yeast. Further, de-suppression of NAT-rRNA in RNAi mutants was validated by qPCR (Fig.5C). For instance of *ago2Δ*, NAT-rRNAs increased by nearly 7-fold in qPCR which was consistently evident in Northern blots. Similar increase was seen for *dcr2Δ*. This Dcr2-Ago2 pathway deviated from the main pathway taken by regular siRNAs biogenesis and transgene-evoked RNAi, in which Dcr1/Ago1

was the major player (Fig.1D). Taken together, we demonstrated a seesawing relationship between 25S rRNA and its complementary NAT-rRNAs in RNAi mutants, which supports the view that rRNA duplexes might form between rRNAs and the NAT-rRNAs to cause rRNA degradation in RNAi mutants via likely RNase IIIs or exosomes. Therefore, RNAi machinery forms a defense system for rRNAs from the formation of RNA duplex by knocking down the NAT-rRNAs.

Functional defects in ribosomes in the RNAi mutants

Disruption of 25S rRNA level in RNAi-deficient mutants may cause functional impairments in ribosomes. This may explain the result shown in Fig. 1A-C, *i.e*. RNAi mutants exhibited hypersensitivity to ribosome inhibitors. We found more defective phenotype of the mutants related to ribosome function, *e.g*. the synthesis of proteins remarkably dropped in RNAi mutants (Fig.6A, S5A). Further, in *E. coli*, *S. cerevisiae* and *A. thaliana*, ribosomal damages result in sensitivity to cold temperature (2,15,32). We then test whether our RNAi mutant yeasts had a similar phenotype. We found that RNAi mutants grew severely slower at low temperature (4℃) than the wild type, though they had a similar growth at 30℃ (Fig. 6B, S1A). When inhibitors and low temperature were jointly applied, the growth was substantially worsened (Fig. S5B). These results confirm again that loss of RNAi machinery causes impairments in ribosome functions.

Discussion

To explore the biological significance of RNAi machinery in the basidiomycetous yeast *C. neoformans*, we conducted extended search for phenotypic change in the mutants of RNAi pathways. We found that disruption of any members in the pathways consistently caused defective phenotype of ribosomes, including hypersensitivity to ribosome inhibitors (Fig. 1A-C), growth retardation under lower temperature and diminished protein biosynthesis (Fig. 6A,B). This finding for the first time establishes a link of RNAi machinery to ribosome function. Indeed, as we demonstrated, RNAi machinery plays a protective role in rRNA (25S rRNA) security and the ribosomes in this yeast. Loss of the RNAi pathways led to a significant decrease of 25S rRNA (Fig. 5A), which might be accounted by the diminished 25S rRNA.

To illustrate the underlying mechanism of the defects in RNAi mutants, we obtained the first significant result of this study, namely, the discovery of a novel class of endogenous sirRNAs, which demonstrated rRNAs could be the substrate for RNAi machinery, given that they are hardly found due to heavily modifications and are associated with ribosomal proteins. Importantly, the finding ascertained that sirRNAs are products of RNAi machinery and refuted the view that they are random degraded products. In a larger sense, existence of sirRNAs in *C. neoformans* provides definitive evidence for the presence of RNAi-generated siRNAs in eukaryotic cells (20).

sirRNAs possess unique structure features, *i.e*. a shorter length (~ 19–20 nt) and a preference of C at 5’ end rather than a U of regular siRNAs (Fig. 2A-D). Notably, approximately 26% of the sirRNAs starts with a sequence of 5’CCT (Table S6). Particularly, two sirRNAs, 001 and 006, possessing the largest reads of all sRNAs, accounting for 35.99% and 3.53% of the total, respectively (Table 1). Their homogeneity of length

and the high abundance were verified by Northern blotting (Fig. 3B&C). Also, production of sirRNAs 001/006 were conserved in var. *grubii* H99, though in a lower level (Fig. 3B). Given the fact that *C. neoformans* also produced a large number of regular siRNAs from non-rRNA sources (Fig. 2), the discovery of sirRNAs suggests that novel mechanism is responsible for their biogenesis. In the meanwhile, there might be an unknown means controls the predominant production of sirRNAs 001 and 006 among the great number of sRNAs in the strain JEC21.

Another interesting fact about sirRNAs, 001/006, is their close location on an internal region of 25S rRNA separated only by a 4-nt spacer. As predicted (Fig. 3A), sirRNAs 001 and 006 have a potential to form an intracellular stem-loop structure which is analogous to the precursor of miRNAs in animals (1), thus might serve as a precursor of sirRNAs. Despite we have no evidence for this hypothesis, we still found that sirRNAs 001 and 006 shared a common precursor, the 120-nt pro-sirRNA (Fig. 3C), which is close to the size of the predicted stem-loop region, indicating this structure may play a role in the origination of the 120-nt precursor.

A critical experiment of this study is the silencing assay for sirRNAs, 001/006. Through the use of reporters, the *URA5* and *CLC1* that were fused accordingly with the complementary sequences of sirRNAs 001 and 006 (Fig. 4A), we demonstrated that sirRNAs 001/006 could trigger RNAi on the mRNAs of transgenic reporters (Fig. 4A-E). This result suggests that as endogenously produced sirRNAs, their intracellular concentration and accessibility to RNAi machinery could assure the occurrence of RNAi reaction. Additionally, the result prompts us that sirRNAs-guided RNAi may plays a role in silencing the invasive nucleic acids, *e.g.* the rDNA or rRNAs. Conceivably, fungi are exposed to nucleic acids in the living niche.

A key finding of this study is the identification of the natural antisense transcripts (NATs) from the rDNA region (as NAT-rRNAs) in this yeast (Fig. 5B, Fig. S4D). NATs are commonly present in eukaryotic cells, though NAT-rRNA is rarely attended (30, 34). NATs can block the transcription of sense RNAs and also are able to form double stranded RNA molecules causing the later to be destroyed (30). We believe that NAT-rRNAs in our yeast might create comparable nuisance to rRNAs, thus become the intracellular targets of sirRNAs-mediated RNAi. HT-seq data attested that there was a group of conventional siRNAs, *i.e.* a-sirRNAs, corresponding to the sequences of NAT-rRNAs, supporting our hypothesis (Fig. 2E,6D). We can see that a-sirRNAs showed a typical siRNA structure, *i.e.* overwhelmingly they had a U at 5' end and a length of 22-nt (Fig. 2E), suggesting they were products of RNAi reaction. Still more, in the wild type, NAT-rRNAs was hardly detectable by Northern blots, but was dramatically accumulated in RNAi mutants (Fig. 5B&C), confirming the RNAi machinery inhibits the expression of NAT-rRNAs. Taking into account of all the results (Fig. 2E, Fig. 4A-E and Fig. 5A), the reverse tendency of alteration in level between 25S rRNA and its NAT-rRNAs suggests sirRNAs guide RNAi machinery against the expression of NAT-rRNAs.

Therefore, we propose a model on the RNAi events in maintaining the 25S rRNA homeostasis to protect ribosome function (Fig. 6C,D). The events include the biogenesis of sirRNAs 001/006, the defense of 25S rRNA against the attack of NAT-rRNAs, and rRNA/NAT-rRNA duplex formation in RNAi mutants. The 25S

rRNA molecules form intramolecular stem-loop structure around the locus of sirRNAs 001/006 as shown in Fig. 3A. An undefined process is responsible for the primary processing of 25S rRNA to generate the shared 120-nt pro-sirRNAs (Fig. 3C, 6C). RNAi pathways are excluded for this stage as we discussed. The shared pro-sirRNAs is split into two major pri-sirRNAs 001 and 006, 55-nt and 60-nt, respectively leading to the birth of 001 and 006 via divergent routes. In this second stage, we can see that RNAi machinery and additional unidentified nucleases could independently finished the split, because in the double mutants, *dcr1dcr2Δ*, *ago1ago2Δ*, the two pri-sirRNAs were still detected (Fig. 3C). Then comes the final stage. The pri-sirRNAs are separately processed to the final products sirRNAs 001 and 006 by RNAi machinery alone. The intermediate products, 33-nt and 35-nt pre-sriRNAs, are formed one step before sirRNAs. Importantly, it is clear that each individual components of the machinery is essential in the final stage. Disruption of any one of them, the Rdp, the Dcrs and Agos, the yeast failed to produce pre-sirRNAs and lost the large part of sirRNAs (Fig. 3B), suggesting the components of RNAi machinery act in a cooperative manner (Fig. 6C). On the other hand, when RNAi pathways are disrupted, accumulated NAT-rRNAs and rRNAs form RNA duplex molecules which are loaded to an RNA duplex scavenging apparatus (RDSA) for degradation by exosomes or Rnt1 (4, 14, 21), and thus, causes the drop of rRNAs and the impairment of ribosomes (Fig. 5A; Fig. 6D). By this model, we present an explanation for the reason why loss of RNAi machinery caused the loss of rRNAs and defects in ribosome function (Fig. 6C,D).

As we mentioned in the section of Results, sirRNAs could be generated by multiple pathways in the wild type. A subgroup of sirRNA001/006 in *rdp1Δ*, *i.e.* accounting for 29.43% of sirRNAs 001, by reads, and 15.98% of 006, were generated by Dcrs or/and Agos (Lane *rdp1Δ*, Fig. 3B-D, Fig. 6C). Actually, HT-seq data suggests that there are at least three isoforms of sirRNAs 001 and 006, respectively (Table 1), and supports the view that multiple biosynthetic mechanisms are involved. When we disrupted both copies of Dcrs or Agos, a trace amount of sirRNAs 001 and 006 were still seen in Northern blots (Fig. 3B,C), manifesting additional pathways are present, for instance, the RNase III family nucleases Rnt1 which is able to cleave double-stranded RNA duplex (14, 21). In the genome of *C. neoformans*, there are three more copies of RNase IIIs apart from the two Dcrs. They might be able to contribute to the production of sirRNAs 001/006. Analyzing their roles in the biogenesis of sirRNAs and RNAi is undergoing. Notably, the short Rdp-independent pathways bypassed the step of pre-sirRNA generation. The pre-sirRNAs, the 33-nt and 35-nt bands, were hardly detectable in *rdp1Δ* (Fig. 3B, C). Whether the three isoforms in Table 1 are accordingly produced by the three proposed pathways is an intriguing question.

Our data disclosed that the long RNAi pathway (Rdp, Dcrs and Agos) was responsible for the RNAi-mediated NAT-rRNA suppression (Fig. 5A-C) and produce a-sirRNAs (Fig. 2E). Besides, HT-seq data showed that disruption of Rdp demolished the generation of a-sirRNAs (Fig. 2E). Thus, Rdp amplification is necessary to initiate RNAi against NAT-rRNA targets. The structure of a-sirRNA, 5'U and 22 nt of the average size, suggests they are RNAi products. Based on qPCR results, we deduced that Dcr2/Ago2 and Rdp play a major role in this suppression process on NAT-rRNAs (Fig. 5B,C, Fig. 6D).

Northern blots clearly demonstrated that Rdp was involved in the third stage of sirRNAs generation (Fig. 3B,C). In *rpdΔ*, the pre-sirRNAs were barely detected by Northern blots, as well as sirRNAs 001 and

006 dropped sharply (Fig. 3B). The reads of 001 and 006 both decreased by nearly ~ 26-fold (Table 1). The complement strain restored the production of pre-sirRNAs (*rdp1Δ-c*, Fig. 3B). These data clearly demonstrated that Rdp amplification is essential for the generation of pre-sirRNAs in the third stage (Fig. 3C). In other words, sirRNAs 001 and 006 were largely produced from the double-stranded products of Rdp amplification which were then subject to processing by Dcrs and Agos. Thus the mode for the biogenesis of miRNAs in mammalian cells from a stem-loop precursor could be excluded in sirRNAs genesis in *C. neoformans*. Nonetheless, the predicted intramolecular stem-loop structure around the sirRNAs 001/006 locus might be required for cleavage in the first stage (Fig. 3A,C). The predicted precursor, sized at ~ 108 nt, is close to the 120-nt pro-sirRNAs (Fig. 3C). Apparently, the 120-nt rRNA band in Fig. 3C harbors both sequences of sirRNAs 001 and 006, as it was hybridized by the probes. Northern blots suggested that the stem-loop structure was cleaved together in the first stage before the subsequently split by Dcrs to form the main pri-sirRNAs, the 55-nt and 60-nt precursors (Fig. 3C). By secondary structure, this stem-loop structure remarkably resembles that of the miRNA precursors in metazoans (1). Additionally, as sirRNAs 001 and 006 have a potential in pairing with each other, thus, they might serve each other the primer in Rdp amplification of pro- and pri-sirRNA templates, giving rise to an ultra-large amount of sirRNAs 001 and 006 (Table 1, Fig. 3B,C).

The rise of RNAi in evolution is still a puzzle. The existence of sirRNAs and a-sirRNAs in *C. neoformans* probably represents an ancient mode of siRNAs and RNAi. Actually, except the random degraded fragments, several types of sRNAs derived from either rRNAs or NAT-rRNAs are previously described in some lower eukaryotes, though they show difference in aspects from sirRNAs of our yeast. Abnormal rRNAs induced by DNA mutagens generates qiRNAs in *N. crassa* (22). Antisense rr-siRNAs and risiRNAs from abnormal rRNAs were found in mutants of RNA turnover pathway in *S. pombe* and *C. elegans* (3, 34). These small rRNAs overwhelmingly have a structure of classic siRNAs, and they are not involved in maintaining rRNA homeostasis and ribosome function. The presence of sirRNAs in our yeast suggests a relatively unique mechanism of siRNA biogenesis with rRNAs. Considering the nature of rRNAs, additional protein factors or pathways besides the core members of the canonical RNAi machinery should be involved as we speculated (Fig. 6C). Indeed, a few novel participants are reported in *C. neoformans* (4). To identify extra members for sirRNA biogenesis could help with complete illustration of how the biogenesis of sirRNAs is originated from the canonical ones, the siRNAs, or verse versa, in *C. neoformans*.

It is noteworthy that loss of RNAi pathways renders the yeast hypersensitivity to low temperature (Fig. 6B,S5B). This defective phenotype not only raises a question about the mechanism for further investigation, but prompts us that RNAi machinery may affect the geographical distribution of *Cryptococcus* as well. It is known that *C. gattii* lacks of the whole RNAi pathways and is primarily prevailing in subtropical and tropical regions (19, 27). A strain of *C. gatti* group VGII isolated from southern China that lacks of RNAi pathway showed hypersensitive to low temperature (retarded growth at 4°C) (Fig. 6E).

The identification of sirRNAs raises several questions. For instance, endogenously produced sirRNAs may participate in regulation of gene expression, similar to siRNAs or miRNAs in complex organisms. Another

question is whether they play a role in maintaining genome stability by suppressing mobility of selfish DNA elements (4, 31). It is also intriguing to think that the defense function of sirRNAs-mediated RNAi may also be a barrier against invasive rRNAs. The fungi in the environment are exposed to the extracellular rRNAs which perchance are readily taken as nutrients. A defense system against foreign rRNAs could a blessing given that foreign rRNAs could be transformed into complementary RNA molecules by Rdp which may disturb the function of rRNAs and ribosomes. Lastly, *C. neoformans* is a widely distributed saprophytic fungus. Secreted sirRNAs by *C. neoformans* may affect the ecology of microbes, or the genetics of plant and mammalian hosts. In the past years, fungal siRNAs have been proven to cause trans-kingdom RNAi and affect gene expression in plant hosts (16, 29).

Materials And Methods

Strains and media

The yeast strains used in this study are listed in Table S1. YPD (2% glucose, 2% bacto-peptone, 1% yeast extract) was the medium for routine growth of *C. neoformans* var. *neoformans* JEC21, var. *grubii* H99 and C. *gattii*, *S. pombe* and *S. cerevisiae*. YNB (2% glucose, 0.17% yeast nitrogen without amino acid and ammomium sulfate, 0.5% ammomium sulfate) was used as minimal media for selection. MIN agar (YNB agar contains 100 μg/mL hygromycin B) and MINFOA agar (YNB agar contains 100 μg/mL hygromycin B, 1 mg/mL 5-fluoro-oroticacid (5-FOA) and 50 μg/mL uracil) were used to grow uracil auxotroph. Asparagine agar (Asn, 0.1% glucose, 0.1% asparagine, 0.3% KH2PO4; pH 5.2) was used for melanin biosynthesis observation in the presence of the laccase substrate nor-epinephrine (NE, 100 mg/liter). Strains were incubated at 30°C for routine growth with or without shaking for 24-72 h.

Stress and antifungal drug sensitivity test for RNAi mutants

Yeast strains (Table S1, the wild-type strain JEC21, *dcr1Δ* (NE473), *dcr2Δ* (NE475), *dcr1Δdcr2Δ*, *ago1Δ*(NE465), *ago2Δ*(NE468), *rdp1Δ*(NE493) and *ago1Δago2Δ*) were grown shaking at 200 rpm in liquid YPD for 18h at 30 ℃. Approximately $2x10^7$ cells were taken and conducted 10-fold serial dilution ($2x10^5$dilutions), and spotted (5 μl of dilution) on YPD agar containing the indicated concentration of 18 μg/ml hygromycin B (HygB), 6 μg/ml G418, 30 μg/ml anisomycin. Cells were incubated at 30 °C for 3~5 days, or at 4 ℃ for 30 days.

Total RNA isolation

To prepare total RNAs, yeast strains were grown in YPD medium at 30 ℃ for 18 h. Approximately 5.0 g yeast cells was collected and washed 3 times by wash buffer (0.1 M EDTA, 0.5 M sodium chloride) at 4℃. Cells were broken by equal volumes 0.1-0.6 mm glass beads and Bullet Blender Storm 24 (Next Advance, USA) for 3 min. Total RNAs were extracted using the RNAiso Plus Kit (Takara Code NO.9108, Dalian, China) according to the supplier's protocol. RNA quality and concentration were detected by POLARstar Omega (BMG Labtech, German).

High throughput sequencing (HT-seq) of small RNAs

Two sets of sRNAs (18-30 nt) were prepared from vegetative grown yeast culture of strains, the wild type JEC21 and mutant *rdp1Δ*. Total RNA was subject to fractionation by PAGE. The band of sRNAs between 18 and 30 nt was cut from the gel, and recovered. sRNAs libraries were constructed for sequencing by BGI (Shenzhen, China) on Illumina Hiseq 4000 platform. Sequencing was carried out in triplicate for each strain. The data size of each sample was 10 Gigabytes. Reads map to genome (https://www.ncbi.nlm.nih.gov/genome/?term =JEC21) by SOAP or Bowtie for following analysis.

Sequence tags from HT-seq went through data cleaning analysis to obtain cleaned sequence of sRNAs. The standard analysis annotated the clean reads into different categories. Those could not be annotated to any category were predicted as the novel siRNA (*i.e.* miRNA annotated in database with reference to plant and animal database by BGI, since none miRNA database for fungi). Target prediction, differential expression, cluster analysis, GO enrichment and KEGG pathway for target genes were analyzed. Apart from conventional analysis, bioinformatics analysis was conducted separately for small RNAs produced from rRNAs (sirRNAs). The BGI provided customized analysis of sirRNAs length distribution, first nucleotide bias and source analysis, in parallel to conventional analysis for siRNAs.

Bioinformatics analysis of small rRNA sequences

Low quality reads and contaminant reads in raw data were removed by a commercial Perl script (BGI, China). Clean reads were then mapped to rRNA genes of *C. neoformans* JEC21 by Blastn, allowing up to one mismatch. rRNA genes of *C. neoformans* JEC21 were identified using Ensemblefungi (http://fungi.ensembl.org/*Cryptococcus neoformans*/Info/Index). Clean reads were also mapped to genome of *C. neoformans* JEC21 in GenBank (https://www.ncbi.nlm.nih.gov/genome/?term =JEC21) to generate IGV files, allowing only perfect matches.

Northern blotting analysis for sirRNAs

Approximately 20 μg RNA samples were resolved in 17% denaturing polyacrylamide gel, which was then stained using SYBR Gold (ThermoFisher Scientific, USA) for 20 min. RNA was transferred to Magna Nylon Transfer Membrane N+ (PALL, German) using semi-dry transferring apparatus (JUNYI Electrophoresis, China). Gel was stained for another 20 min to check transfer efficiency. EDC solution (0.16M 1-ethyl-3-(3-dimethylaminopropyl) carbodiimide was prepared in 0.13 M 1-methylimidazole, pH 8.0) to crosslink sRNA to membrane at 60℃ for 1h. Synthesized oligos (All oligos used in this study and their location on templates are listed in Table S2) corresponding to target sRNAs were labeled with γ-[32P] ATP (PerKinElmer, USA) using T4 polynucleotide kinase (Takara, Dalian, China). The membrane was pre-hybridized using Ambion® ULTRAhyb®-Oligo (ThermoFisher Scientific, USA) for 30 min and hybridized after addition of probes overnight at 37℃. The membrane was washed once by washing buffer (2xSSC, 0.2% SDS) for 10 min at room temperature. The membrane with a film was incubated in a dark cassette for 7 days as indicated at -80℃. The film was exposed using Optimax2010 (ProTec, German). All the sequences of probes and primers are listed in Table S2.

Quantitative PCR

Reverse transcription of total RNA was conducted by One-Step gDNA Removal and cDNA Synthesis SuperMix (Transgen, Beijing, China) according to the protocol. For determination of mRNAs of reporter genes or the level of rRNA and AS-rRNA: 2 μg total RNA was treated by the Kit in a volume of 20 μl reaction system for 15 min at 42 ℃, and 5 seconds at 85 ℃. Original cDNA was diluted by 10-folds for subsequent quantitative PCR. For antisense and sense 25S rRNA assay, gene specific primers of 25S rRNA and actin were used instead of random primers (Table S2).

Quantitative PCR (qPCR) was conducted by two PCR systems. For rRNA, LightCycler 480 II and correspondent LC 480 SYBR Green I Master (Roche, Switzerland) were employed. A PCR reaction contains 10 μl 2x Master Mix, 1μl forward/reverse primers (10 μM), 1 μl cDNA and 7 μl ddH2O. For other assays, ABI 7500 Real-Time PCR System (Thermo-Fisher Scientific, USA) and SuperReal PreMix Plus SYBR Green (Tiangen, China) were used. A PCR reaction includes 10 μl 2x SuperReal PreMix Plus, 0.6 μl forward/reverse primers (10 μM), 0.4 μl 50x ROX, 1 μl cDNA and 7.4 μl ddH2O.

Each reaction was conducted in triplicate, non-RT RNA was used as template as negative control reaction and actin mRNA was utilized as reference. Specificity of every pairs of primers was validated by checking the melting curves. $2^{\Delta\Delta Ct}$ method was employed to calculate expression levels of target genes in this study.

Reporter construction and silencing assay

The *Cryptococcus* genes *URA5* and *CLC1* were utilized as the targets of sirRNAs in silencing assay by following the protocol (18). *URA5* encodes an enzyme in the biosynthesis of uracil. *URA5*-knockdown strain would yield partial auxotrophic phenotype for uracil and is tolerant to toxin 5-fluoro-oroticacid (5-FOA), which is lethal to the wild type. *CLC1* encodes a chloride channel that is required for pigmentation in *C. neoformans*. Knockdown transformants produce a phenotype of lighter pigmentation on the laccase substrate nor-epinephrine (NE)-containing plates, which would be similar to TX1(*clc1Δ*). The two genes were respectively ligated to the reverse complementary sequence of 001 or 006 at 3' UTR as the recognition site of 001/006 (Figure 3C). For negative control in *URA5* test, B4500FOA (JEC21 *ura5Δ*), a uracil auxotroph, was transformed with *URA5* alone (CT, Fig. 4B). Negative control in *CLC1* Test was *rdpΔ* hosting the recipient of CLC-sirRNA cassette, and strain TX1 (JEC21 *clc1Δ*) was also displayed. Transformants were randomly picked for analysis in each transformation. YNB was used as minimal medium. Transformants were selected on YPD plates containing 100 mg/ml hygromycin B. And single colonies were obtained by streaking.

The silencing cassette was constructed by following the description (18). Briefly, for *URA5* reporter, native copy of *URA5* from JEC21 including the promotor and coding sequence (CDS) region was PCR amplified with the primers URA5-ORF-Kpn I and URA5-ORF-Bgl II (Table S2). *URA5* terminator was fused to the complementary sequence of sirRNA-001 or sirRNA-006 by PCR after the stop codon with the primers URA5-srRNA006-Bgl II/URA5-srRNA001-Bgl II and URA5-ter-Hind III. The *URA5* promotor and ORF, and

URA5 sirRNA-terminator were simultaneously ligated to vector pBS-HYG. The final plasmids were linearized and transformed to B4500FOA (JEC21 *ura5Δ*) or other recipients by electroporation. In order to detect expression level of *URA5* gene, three randomly selected transformants and two control strains were grown on YNB and YNB (supplemented with 1 mg/mL 5-FOA) for phenotype analysis.

Similarly, primers CLC1-ORF-Kpn I and CLC1-ORF-Bgl II were used for amplification of the promoter and ORF of *CLC1*. For fusion of *CLC1* terminator with the complementary sequence of sirRNA 001 or sirRNA 006, the primers, CLC1-srRNA006-Bgl II/ URA5-srRNA001-Bgl II and CLC1-ter-Hind III, were used. The *CLC1* promotor, ORF, and *URA5* terminator were simultaneously ligated to pBS-HYG, which was linearized and transformed to TX1 strain by electroporation. To check expression level of *CLC1* gene, two randomly purified transformants and one control were grown on Asn agar supplemented with NE for pigmentation assay (18).

Determination of total protein biosynthesis

To examine the production of total proteins, strains were cultured in YPD medium for 18h at 30℃.Approximately 0.1 g yeast cells was washed by double-distilled water for 3 times at 4℃. Fungal cells were broke by equal volumes 0.1-0.6-mm glass beads and Bullet Blender Storm 24 (Next Advance, USA) for 1min by 4 times. Total proteins and DNA were extracted respectively using the RIPA (Applygen C1053, Beijing, China) add Protease Inhibitor (MCE HY-K0010) or TENTS(1 mM pH8.0 EDTA·2Na, 10 mM pH7.5 Tris·HCl, 1% SDS, 2% Triton X-100) according to the reagent instruction. Total protein quality and concentration were detected by BCA Kit (Applygen Technologies, Inc, Beijing, China). Genome quality and concentration were detected by Microplate Reader (BioTek, Synergy H1). Capacity of protein biosynthesis was expressed as ratio of proteins to DNA in each strains. Each sample was prepared in parallel in triplicate.

CRISPR-Cas9 editing system to create double knock-out mutants

To effectively target genes in *C. neoformans* JEC21, we used a suicide CRISPR-Cas9 protocol created for JEC21 (28). In brief, to generate gRNA in vivo, we cloned the N19 target sequence from aim genes into the CRISPR plasmid pRH003 using the BspQI (NEB R0712S) restriction enzyme. We designed a CRISPR-containing plasmid to disrupt the target gene flanking the *URA5* marker. The CAS9 and gRNA cassettes would be degraded once double crossover was initiated by Cas9 at the gRNA target site. Thus, we amplified an approximately 1-kb fragment upstream and downstream of target genes using the corresponding primers (Table S2). We linearized the final design with In-Fusion HD Cloning Kits (TAKARA 639538). The In-Fusion enzyme could fused DNA fragments efficiently and precisely by recognizing the 15-bp overlaps at the ends.

Southern blotting for double mutants of RNAi pathways

Southern blotting verified that both *ago1Δago2Δ* and *dcr1Δdcr2Δ* had the desired insertion of *URA5* at the targeting exon. *C. neoformans* cells were grown in liquid YPD to stationary phase at 30°C. DNA

extraction was performed according to a standard protocol using glass beads. Genomic DNA was doubly digested with restriction endonucleases, which cut the DNA of the wild type and mutants into different sizes; these fragments were then separated on a 0.7% agarose gel separation. Southern blotting was performed using a DIG High Prime DNA Labelling and Detection Starter Kit II (Roche), according to the user's manual, and the film was exposed using a developing solution and a fixing bath. Thus, we obtained the genes disrupted strain, designated as *ago1Δago2Δ* and *dcr1Δdcr2Δ* respectively. We chose the verified mutants for further analyses.

References

1. Bartel DP., Metazoan MicroRNAs. Cell **173**, 20–51 (2018).
2. Bayliss FT., J. L. Ingrahm, Mutation in *Saccharomyces cerevisiae* conferring streptomycin and cold sensitivity by affecting ribosome formation and function. J Bacteriol **118**, 319–328 (1974).
3. Buhler M., N. Spies, D. P. Bartel, D. Moazed, TRAMP-mediated RNA surveillance prevents spurious entry of RNAs into the *Schizosaccharomyces pombe* siRNA pathway. Nat Struct Mol Biol **15**, 1015–1023 (2008).
4. Burke JE, *et al*. A Non-Dicer RNase III and Four Other Novel Factors Required for RNAi-Mediated Transposon Suppression in the Human Pathogenic Yeast *Cryptococcus neoformans*. G3 (Bethesda). 2019 Jul 9;9(7):2235–2244. doi: 10.1534/g3.119.400330. PMID: 31092606; PMCID: PMC6643885.
5. Carthew RW., E. J. Sontheimer, Origins and Mechanisms of miRNAs and siRNAs. Cell **136**, 642–655 (2009).
6. Chang SS, Zhang Z, Liu Y. RNA interference pathways in fungi: mechanisms and functions. Annu Rev Microbiol. 2012;66:305 – 23. doi: 10.1146/annurev-micro-092611-150138. PMID: 22746336; PMCID: PMC4617789 (2012).
7. Claycomb JM., Ancient endo-siRNA pathways reveal new tricks. Curr Biol **24**, R703-715 (2014).
8. Cogoni C., G. Macino, Gene silencing in *Neurospora crassa* requires a protein homologous to RNA-dependent RNA polymerase. Nature **399**, 166–169 (1999).
9. Carrington JC., V. Ambros, Role of microRNAs in plant and animal development. Science **301**, 336–338 (2003).
10. Drinnenberg IA, Fink GR, Bartel DP. Compatibility with killer explains the rise of RNAi-deficient fungi. Science. 2011 Sep 16;333(6049):1592. doi: 10.1126/science.1209575. PMID: 21921191; PMCID: PMC3790311.
11. Drinnenberg IA. *et al.*, RNAi in budding yeast. Science **326**, 544–550 (2009).
12. Dumesic P. A. *et al.*, Stalled spliceosomes are a signal for RNAi-mediated genome defense. Cell **152**, 957–968 (2013).
13. Ellliott D., M. Ladomery, Ed, *Molecular Biology of RNA (2nd Revised edition)*. (Oxford University Press, Oxford, UK, 2016).

14. Ge D, Lamontagne B, Elela SA. RNase III-mediated silencing of a glucose-dependent repressor in yeast. Curr Biol. 2005 Jan 26;15(2):140-5. doi: 10.1016/j.cub.2004.12.001. PMID: 15668170.
15. Guthrie C., H. Nashimoto, M. Nomura, Structure and function of *E. coli* ribosomes. VIII. Cold-sensitive mutants defective in ribosome assembly. Proc Natl Acad Sci U S A **63**, 384–391 (1969).
16. Huang CY, Wang H, Hu P, Hamby R, Jin H. Small RNAs - Big Players in Plant-Microbe Interactions. Cell Host Microbe. 2019 Aug 14;26(2):173–182. doi: 10.1016/j.chom.2019.07.021. PMID: 31415750.
17. Janbon G. *et al.*, Characterizing the role of RNA silencing components in *Cryptococcus neoformans*. Fungal Genet Biol **47**, 1070–1080 (2010).
18. Jiang N., Y. P. Yang, G. Janbon, J. Pan, X. D. Zhu, Identification and Functional Demonstration of miRNAs in the Fungus *Cryptococcus neoformans*. Plos One **7**, 12 (2012)
19. Kwon-Chung KJ, *et al.*. *Cryptococcus neoformans* and *Cryptococcus gattii*, the etiologic agents of cryptococcosis. Cold Spring Harb Perspect Med. 2014 Jul 1;4(7):a019760. doi: 10.1101/cshperspect.a019760. PMID: 24985132; PMCID: PMC4066639.
20. Lambert M., A. Benmoussa, P. Provost, Small Non-Coding RNAs Derived From Eukaryotic Ribosomal RNA. Noncoding RNA **5**, 16 (2019).
21. Lamontagne B, Larose S, Boulanger J, Elela SA. The RNase III family: a conserved structure and expanding functions in eukaryotic dsRNA metabolism. Curr Issues Mol Biol. 2001 Oct;3(4):71–8. PMID: 11719970.
22. Lee HC, *et al.*. qiRNA is a new type of small interfering RNA induced by DNA damage. *Nature*. 2009 May 14;459(7244):274-7. doi: 10.1038/nature08041. PMID: 19444217; PMCID: PMC2859615.
23. Li D, Zhang X, Li Z, Yang J, Pan J, Zhu X. *Cryptococcus neoformans* Ca(2+) homeostasis requires a chloride channel/antiporter Clc1 in JEC21, but not in H99. FEMS Yeast Res. 2012 Feb;12(1):69–77. doi: 10.1111/j.1567-1364.2011.00763.x. Epub 2011 Dec 13. PMID: 22093100.
24. Thoms M. *et al.*, The Exosome Is Recruited to RNA Substrates through Specific Adaptor Proteins. Cell **162**, 1029–1038 (2015).
25. Torres-Martínez S, Ruiz-Vázquez RM. The RNAi Universe in Fungi: A Varied Landscape of Small RNAs and Biological Functions. Annu Rev Microbiol. 2017 Sep 8;71:371–391. doi: 10.1146/annurev-micro-090816-093352. Epub 2017 Jun 28. PMID: 28657888.
26. Volpe T A. *et al.*, Regulation of heterochromatic silencing and histone H3 lysine-9 methylation by RNAi. Science **297**, 1833–1837 (2002).
27. Wang X. *et al.*, Sex-induced silencing defends the genome of *Cryptococcus neoformans* via RNAi. Gen Dev **24**, 2566–2582 (2010).
28. Wang Y, *et al.*,. A 'suicide' CRISPR-Cas9 system to promote gene deletion and restoration by electroporation in *Cryptococcus neoformans*. Sci Rep. 2016 Aug 9;6:31145. doi: 10.1038/srep31145. PMID: 27503169; PMCID: PMC4977553.
29. Weiberg A, *et al.*, Fungal small RNAs suppress plant immunity by hijacking host RNA interference pathways. *Science*. 2013 Oct 4;342(6154):118 – 23. doi: 10.1126/science.1239705. PMID:

24092744; PMCID: PMC4096153.

30. Werner A, Swan D. What are natural antisense transcripts good for? Biochem Soc Trans. 2010 Aug;38(4):1144–9. doi: 10.1042/BST0381144. PMID: 20659019; PMCID: PMC4284956.
31. Yamanaka S. *et al.*, RNAi triggered by specialized machinery silences developmental genes and retrotransposons. Nature **493**, 557–560 (2013).
32. Yu H. *et al.*, STCH4/REIL2 Confers Cold Stress Tolerance in *Arabidopsis* by Promoting rRNA Processing and CBF Protein Translation. Cell Rep **30**, 229–242 e225 (2020).
33. Zamore P. D., B. Haley, Ribo-gnome: the big world of small RNAs. Science (New York, N.Y.) **309**, 1519–1524 (2005).
34. Zhou X. *et al.*, RdRP-synthesized antisense ribosomal siRNAs silence pre-rRNA via the nuclear RNAi pathway. Nat Struct Mol Biol **24**, 258–269 (2017).
35. Zhu C. *et al.*, Erroneous ribosomal RNAs promote the generation of antisense ribosomal siRNA. Proc Natl Acad Sci U S A **115**, 10082–10087 (2018).
36. Zilberman D., X. Cao, S. E. Jacobsen, ARGONAUTE4 control of locus-specific siRNA accumulation and DNA and histone methylation. Science **299**, 716–719 (2003).

Table

Table 1 is available in the Supplementary Files section

Figures

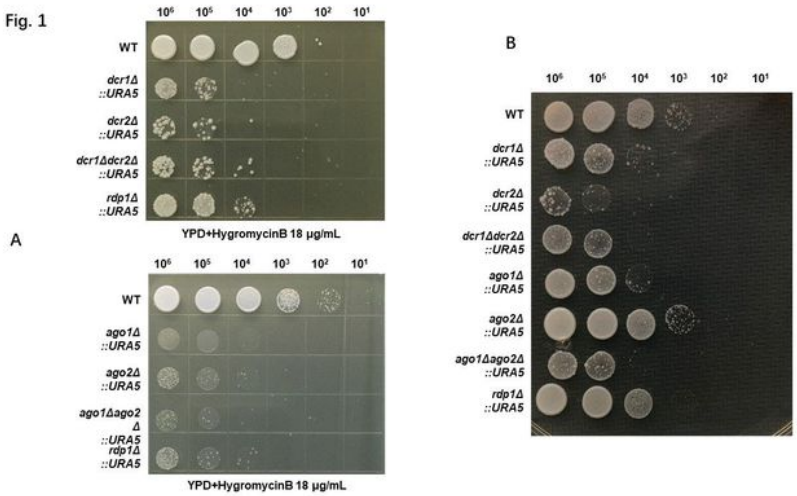

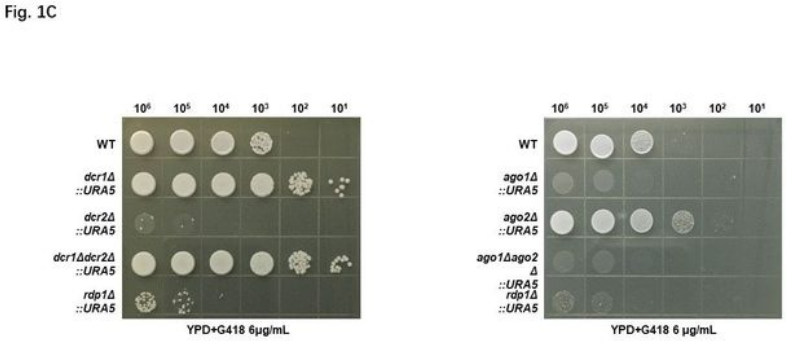

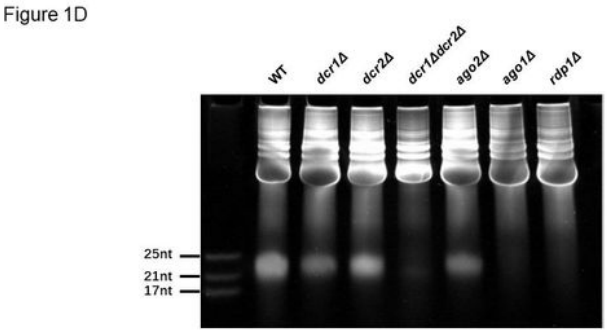

Figure 1

A-**C**. Sensitivity of RNAi mutants to ribosome inhibitors: **A**. Hygormycin B (18 μg/mL), **B**. Anisomycin (30 μg/mL, 5 days), and **C**. G418 (6 μg/mL). Serial dilution of cell suspension of 5 μl was dropped to YPD agar at 30°C for 3 days. Noted: four strains, *agoΔ2*, *ago1Δago2Δ2*, *dcr1Δ* and *dcr1Δdcr2Δ*, were originally created with G418 resistance marker and showed resistant to G418. **D**. PAGE display of RNAi-generated 18-25-nt sRNAs in *C. deneoformans.* Total RNAs was prepared from the wild type (WT) and RNAi

mutants. Samples of RNAs were equalized and ~10 µg was loaded to 15% denaturing PAGE. Ladders are indicated.

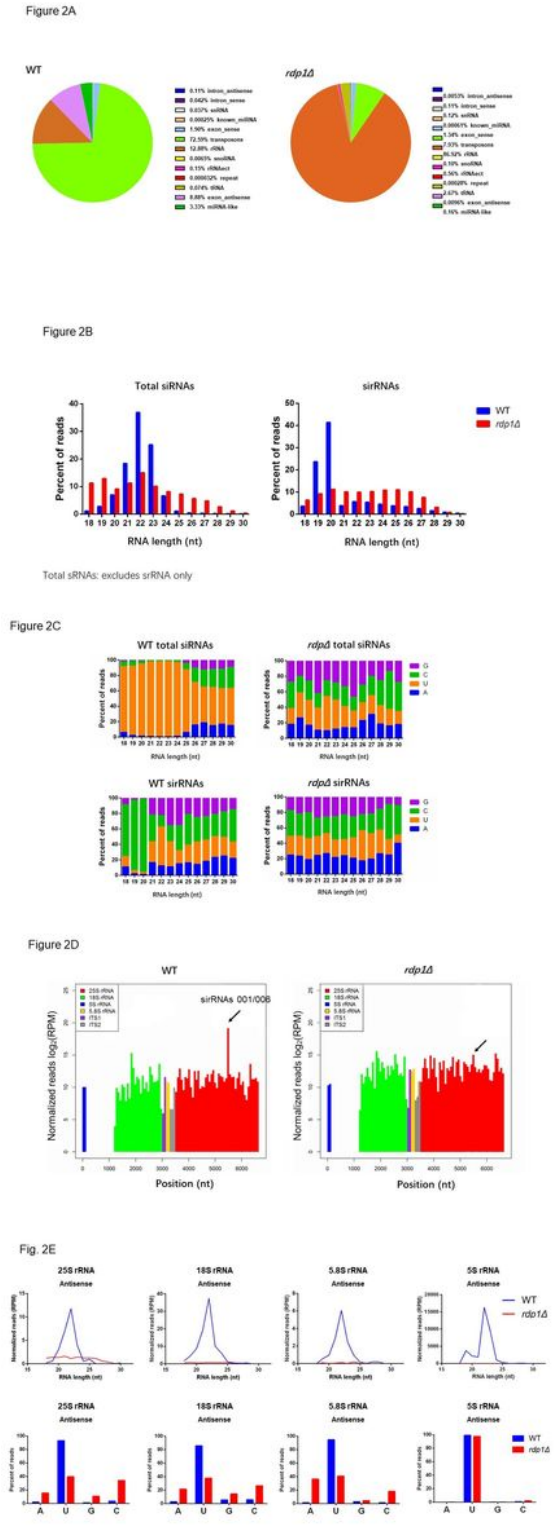

Figure 2

Identification of sirRNAs. HT-seq was conducted in triplicate for strains WT and *rdp1Δ*. Each value was the average of the triplicate (Figure S3-S5). **A.** Pie chart showing percentages by sRNA orgination sources

relative to the total reads of sRNAs (including both siRNAs and sirRNAs). rRNA-derived sRNAs was shown in dark orange which counts for 12.88% of the total (WT, left panel). **B**. Size distribution of classic siRNAs (left) and sirRNAs (right) in both strains, WT and *rdp1Δ*. **C**. 5’ nucleotide bias of siRNAs and sirRNAs. **D**. Distribution of sirRNAs corresponding to rRNAs in normalized reads (RPM) to minimize the background noise arisen from the removal of non-rRNA derived sRNAs in *rdp1Δ* strain. Logarithm of RPM was used as y-axis. The x-axis was diagramed in the sequence of one set of rRNA in *C. deneoformans*. The clustered sirRNA001 and 006 were indicated by arrow. **E**. a-sirRNAs derived from NAT-rRNAs in WT and *rdp1Δ*. Size distribution (Upper) and 5’ nucleotide bias (Bottom), corresponding to the rRNAs as indicated.

Fig. 3A

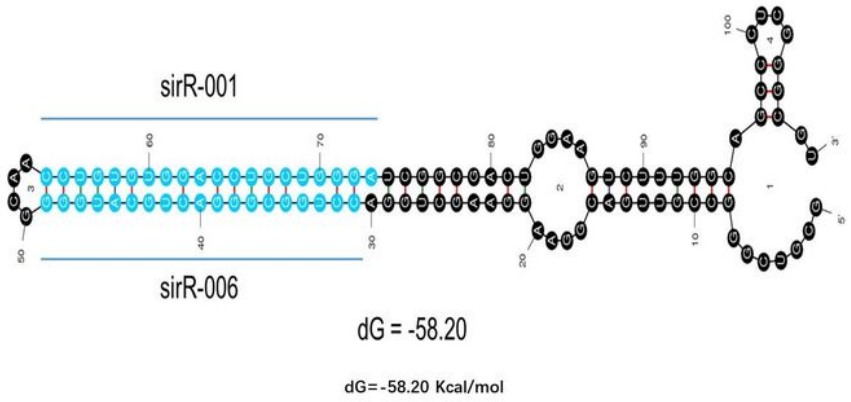

Fig. 3B

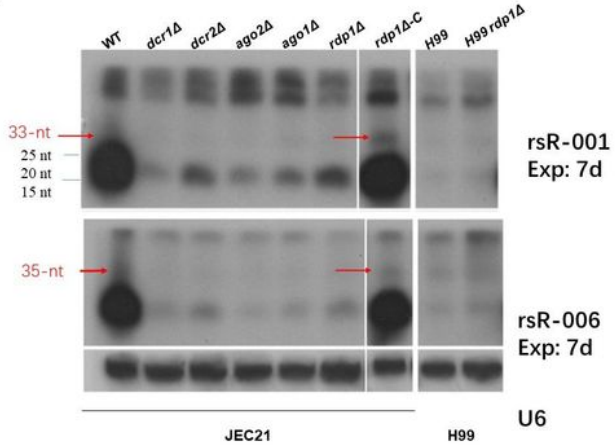

Fig. 3C

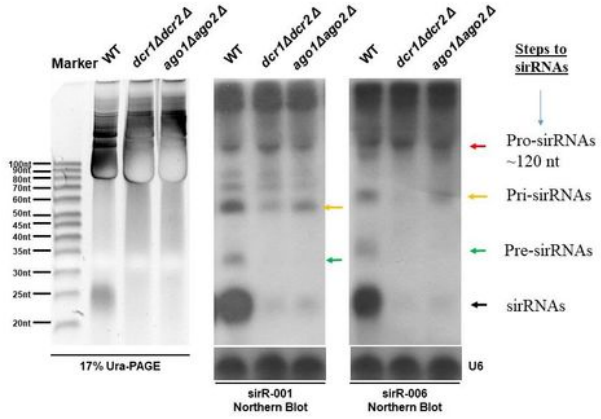

Figure 3

Northern blots for demonstration of RNAi-dependent sirRNAs 001 and 006. **A**. A stem-loop structure covering a 108-nt region flanking sirRNAs, 001 and 006 was predicted by mFold Server. Sequences of 001 and 006 were highlighted in blue. **B.** Northern blots for 001 (upper), 006 (bottom). Precursors, 33-nt of 001, 35-nt of 006 was indicated by red arrows. Samples were equalized to ~10 µg of RNA was loaded to 17% denaturing PAGE. Exposure time: 7 days. Ladders are indicated. The snRNA U6 was used as internal

control. Probed with synthesized DNA sequences complementary to 001 or 006, respectively (Table S2). C. Detection by Northern blots of the precursors of sirRNAs during biogenesis. Details were described in sections of Results and Discussion. The precursors were indicated by colored arrows (right panel). Red, pro-sirRNAs, ~120-nt. Orange, pri-sirRNAs, 55-nt toward 001, 60-nt to 006; Green, pre-sirRNAs, 33 nt and 35 nt, respectively ,toward the generation of 001 and 006. Black, sirRNAs 001 and 006. Northern blots show the precursors produced by were RNAi machinery, except the pro-sirRNAs which were generated by unknown mechanism. The left panel is PAGE. Size of the markers is indicated.

Fig. 4A

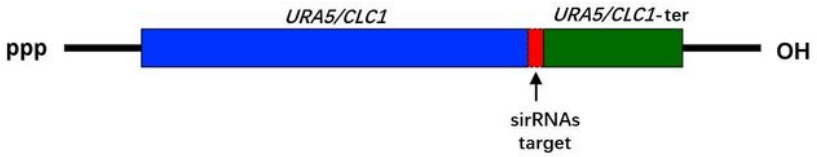

Fig. 4B&C

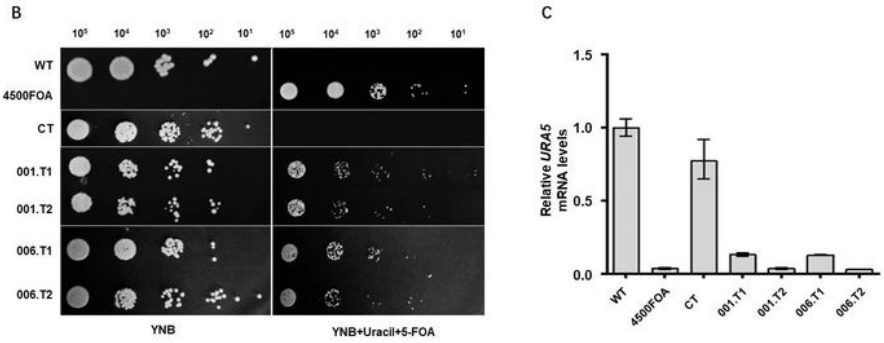

Fig. 4D&E

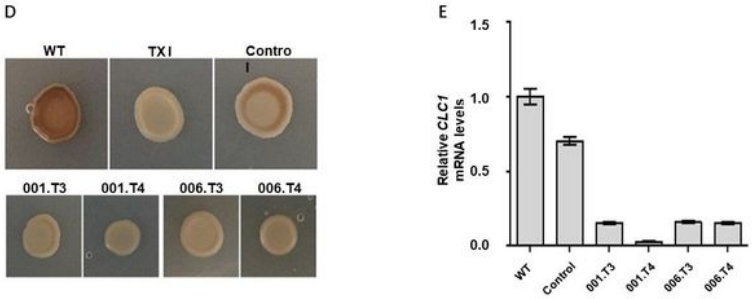

Figure 4

Silencing assay for sirRNAs after the protocol by Jiang et al (18). **A.** Schematic of the reporter cassette. As target, the complementary sequences of sirRNAs (in red) were inserted immediately after the stop codon of the ORF of the reporter genes. **B**. Silencing assay for *URA5-sirRNAs*. Cells were dropped by10-fold serial dilution on YNB or YNB supplemented with drugs, FOA or hygromycin B for selection for transformants, at 30 ℃ for 3 days. Left panel shows inhibited growth of two transformants with 001 and 006 inserts, named in 001.T1, 002.T2, and 006.T1, 006.T2, accordingly. Three strains were set as controls: WT, JEC21. 4500FOA, JEC21(*ura5-*). CT: transformants with the vector containing *URA5* gene only (Materials and Methods). Right panel shows tolerance of transformants to 5-FOA, while WT and CT were killed. **C**. qPCR measurement of *URA5-sirRNAs* mRNA in the transformants. **D**. Silencing assay for *CLC1-sirRNAs*. Strains were grown on Asn containing the laccase substrate nor-epinephrin (NE) to make melanin, at 30 ℃ for 3 days. The upper panels show melanin production in WT, but less in TX1 (*clc1Δ*), and Control strain restored to some extent. The bottom panels show less melanin biosynthesis (lighter color) in transformants with silenced *CLC1-sirRNAs*. **E.** qPCR measurement of *CLC1* mRNA in the transformants. qPCR was performed in triplicate for each strain. The columns depict relative quantity to the wild-type mRNAs. Errors are expressed as standard deviation.

Fig. 5A

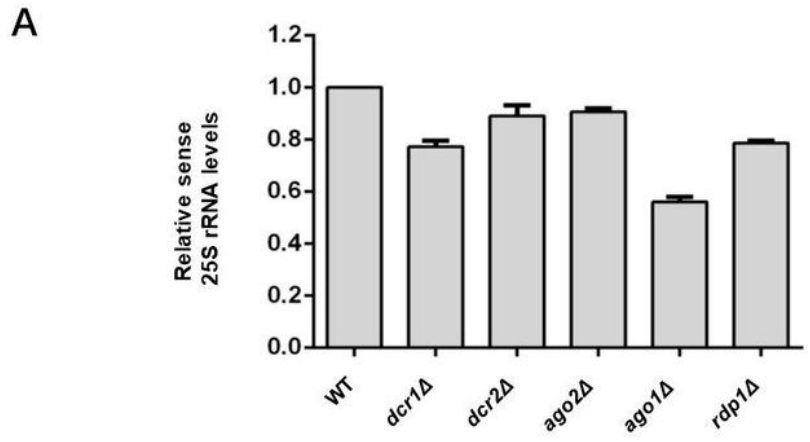

Fig. 5B&C

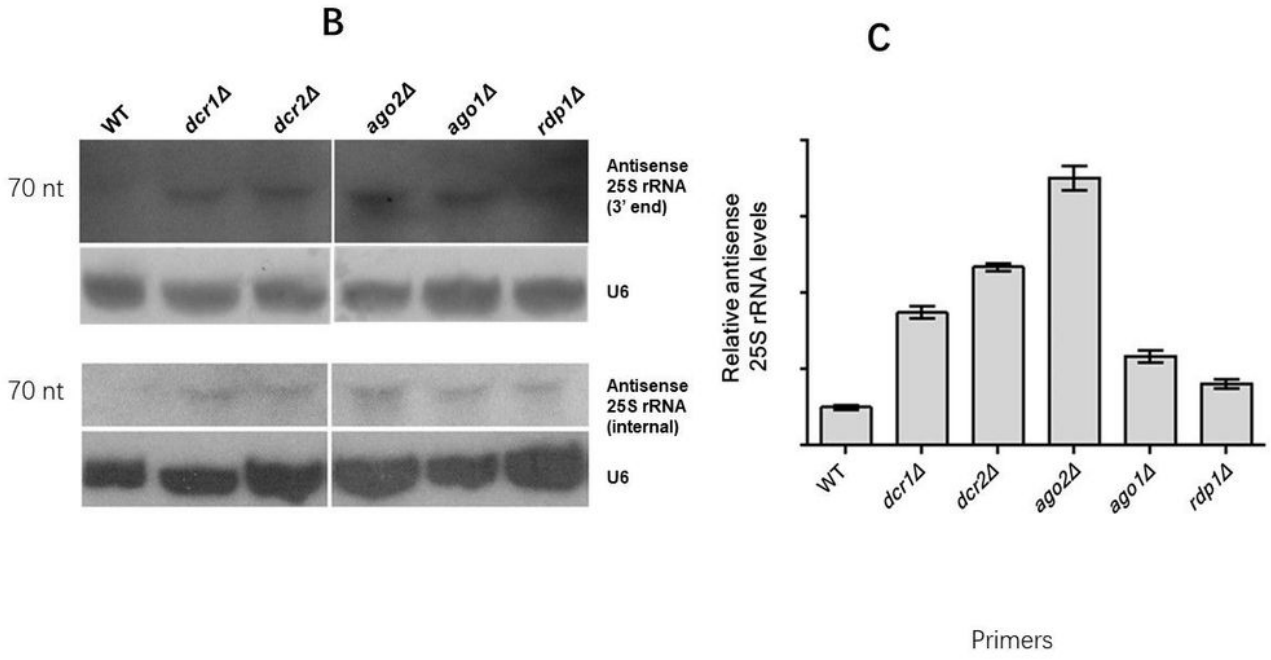

Figure 5

RNAi machinery maintains 25S rRNA level and Suppresses NAT-rRNA. **A**. qPCR demonstration of decreased level of 25S rRNA in RNAi mutants. **B**. Northern blot demonstration of NAT-rRNAs in WT and RNAi mutants. For double examination, two sets of probes mapping to internal and 3’ end of 25S rRNA were independently used (Table S2). 20 μg total RNA was loaded for the blots. U6 as internal control. **C**.

qPCR demonstration of increased NAT-rRNA level in RNAi mutants. Bars show relative quantity to the WT. Reactions wwere performed in triplicate. Errors were expressed as standard deviation.

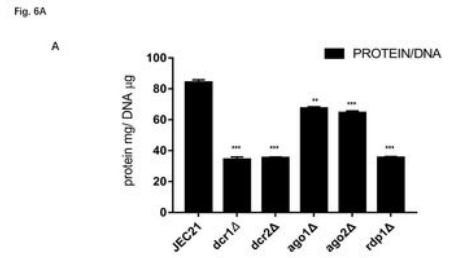

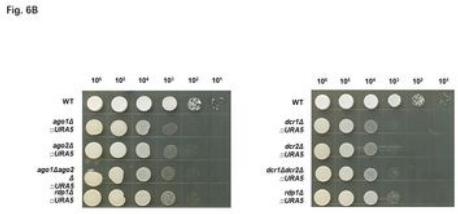

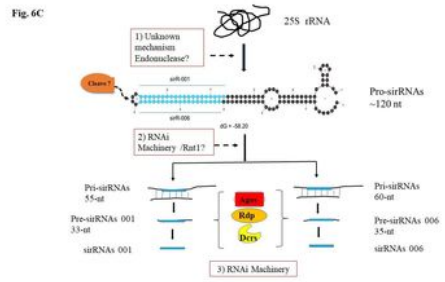

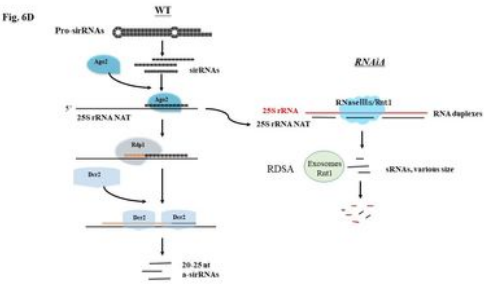

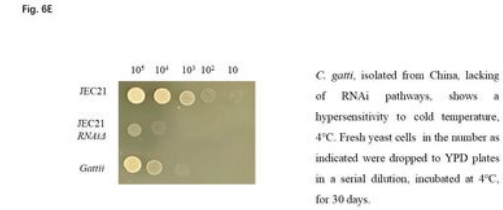

C. gattii, isolated from China, lacking of RNAi pathways, shows a hypersensitivity to cold temperature, 4°C. Fresh yeast cells in the number as indicated were dropped to YPD plates in a serial dilution, incubated at 4°C, for 30 days.

Figure 6

A&B. Functional defects in ribosomes in RNAi mutants. **A**. Dimonished protein biosynthesis in RNAi mutants. **B**. RNAi mutants were sensitive to low growth temperature. Cells dropped to YPD agar at the

number indicated, incubated at 4℃ for 30 days.

C. Schematic of the biogenesis of sirRNAs. The biogenesis process was proposed to include three stages (in red frames). 1) The generation of the 120-nt pro-sirRNAs. 25S rRNA is processed by unknown mechanism which should cover the demodification of rRNAs and cleavage by endonucleases. The pro-sirRNA contains sequences of sirRNAs 001 and 006 (in blue) which putatively form a step-loop structure. 2) The formation of two main precursors leading to sirRNAs 001 and 006, designated as pri-sirRNAs 001 (55 nt) and 006 (60 nt), accordingly. RNAi machinery including Dcr1/2, Ago1/3 and Rdp is involved in this process. Besides, unidentified RNase III nucleases, such as Rnt1 equivalent also contribute to the generation of the intermediates (Fig. 3C). 3) RNAi machinery alone processes pri-sirRNAs into pre-sirRNAs and the final products sirRNAs. Conceivably, Agos load sirRNAs or other siRNAs to the pri-sirRNA templates, which are subject to Rdp amplification to form double stranded RNA molecules which then are cleaved by Dcrs. The pre-sirRNAs may alternatively be trimmed by Agos to form sirRNAs.

D. Mechanism of RNAi machinery in the defense of rRNAs security by suppressing NAT-rRNAs. Ago2/Dcr2 and Rdp are the main players in this process. Left panel shows the rRNA-derived sirRNAs-mediated suppression of NAT-rRNAs by the action of RNAi machinery, in the wild type. The sirRNAs guide Ago proteins, mainly Ago2 in this case to the complementary NAT-rRNA, the natural antisense transcripts of rRNA, Rdp amplified sirRNAs-priming NAT-rRNAs to form RNA duplexes which are subject to digestion by Dcr2, giving rise to 20-25 nt a-sirRNAs. Right panel shows: in RNAi mutants, accumulated NAT-rRNAs form RNA duplexes with rRNAs that are digested by other RNase IIIs, *e.g.* Rnt1, giving rise to random small rRNA fragments which are broken down completely by exosomes or some RDSA for RNA Duplex Scavenging Apparatus.

Supplementary Files

This is a list of supplementary files associated with this preprint. Click to download.

- Table1.pptx
- SupplementaryFiguresXLegends.pptx
- TableS1Strains.docx
- TableS2PrimersXProbes.docx
- SupplementaryTablesS3S5.pptx
- Tab.S6.TotalsirRNAswithreadsover100.xlsx